A genomic duplication spanning multiple P450s contributes to insecticide resistance in the dengue mosquito *Aedes aegypti*

Tiphaine Bacot[1], Chloé Haberkorn[§,1], Joseph Guilliet[§,1,2], Julien Cattel[§,1], Mary Kefi[§,3,4], Louis Nadalin[1], Jonathan Filee[2], Frederic Boyer[1], Thierry Gaude[1], Frederic Laporte[1], Jordan Tutagata[1], John Vontas[3,4], Isabelle Dusfour[5], Jean-Marc Bonneville[#,1], Jean-Philippe David[#,1,*]

# equal contribution
§ equal contribution
* corresponding author

[1] Laboratoire d'Ecologie Alpine (LECA, UMR 5553), Université Grenoble-Alpes (UGA), Université Savoie Mont-Blanc (USMB), CNRS, 38041 Grenoble, France.

[2] Université Paris-Saclay, CNRS, IRD, UMR Évolution, Génomes, Comportement et Écologie, 91198 Gif-sur-Yvette, France.

[3] Institute of Molecular Biology and Biotechnology, Foundation for Research and Technology Hellas, Heraklion, Greece.

[4] Pesticide Science Laboratory, Department of Crop Science, Agricultural University of Athens, Athens, Greece.

[5] Vectopôle Amazonien Emile Abonnenc, Institut Pasteur de la Guyane, Cayenne, France ; Global Health Department, Institut Pasteur, Paris, France.

* jean-philippe.david@univ-grenoble-alpes.fr

Abstract

Resistance of mosquitoes to insecticides is one example of rapid adaptation to anthropogenic selection pressures having a strong impact on human health and activities. Target-site modification and increased insecticide detoxification are the two main mechanisms underlying insecticide resistance in mosquitoes. While target-sites mutations are well characterised and often used to track resistance in the field, the genomic events associated with insecticide detoxification remain partially characterised. Recent studies evidenced the key role of gene duplications in the over-expression of detoxification enzymes and their potential use to track metabolic resistance alleles in the field. However, such genomic events remain difficult to characterise due to their complex genomic architecture and their co-occurrence with other resistance alleles. In this concern, the present work investigated the role of a large genomic duplication affecting a cluster of detoxification enzymes in conferring resistance to the pyrethroid insecticide deltamethrin in the mosquito *Aedes aegypti*.

Two isofemale lines originating from French Guiana and being deprived from major target-site mutations showed distinct insecticide resistance levels. Combining RNA-seq and whole genome pool-seq identified a 220 Kb genomic duplication spanning multiple cytochrome P450s carried by the resistant line. The genomic architecture of the duplicated loci was elucidated through long read sequencing, evidencing its transposon-mediated evolutionary origin. The importance of this P450 duplication in deltamethrin survival was supported by genotype-phenotype association and RNA interference. Experimental evolution suggested that this P450 duplication is associated with a significant fitness cost, potentially affecting its adaptive value in presence of other resistance alleles.

Overall, this study supports the importance of genomic duplications affecting detoxification enzymes in the rapid adaptation of mosquitoes to insecticides. Deciphering their genomic architecture provides new insights into the evolutionary processes underlying such rapid adaptation. Such findings and provides new tools for the surveillance and management of resistance in the field.

Key words: Mosquito; Insecticide resistance; P450; Gene duplication; Kdr mutation; *Aedes aegypti*

30 # Introduction

31 Natural populations experience a wide range of selective pressures, leading to the accumulation of
32 locally adaptive features and the expression of complex phenotypes (Orr, 2005). Among them, those
33 driven by human activities promote novel and strong selective pressures. Understanding the genetic
34 mechanisms allowing populations to quickly respond to rapid environmental changes has become a
35 major goal (Hendry et al., 2008, 2017; Palumbi, 2001). Resistance of insects to insecticides is a key
36 example of rapid evolution under strong anthropogenic selective pressures. This adaptation has
37 occurred quickly and independently in a large number of taxa with frequent parallel trajectories
38 (Ffrench-Constant et al., 2004; Liu, 2015). As a consequence of local and temporal variations of the
39 selection pressures, the genetic modifications affecting resistant populations are often complex and
40 combine several resistance mechanisms that are potentially additive, each of them bringing variable
41 fitness costs. In addition, the very strong selection pressure exerted by insecticides is prone to
42 produce demographic effects. Such complexity makes the identification of resistance alleles and the
43 assessment of their respective contribution challenging (Ffrench-Constant et al., 2004; Li et al., 2007).

44 Besides the understanding of the genetics of rapid adaptation and the origins of complex traits,
45 deciphering the molecular bases of insecticide resistance is also essential for improving pest
46 management strategies (Hawkins et al., 2018). Among taxa of major economic and medical
47 importance, mosquitoes represent a major threat for public health worldwide because of their ability
48 to transmit human viruses and pathogens (Lounibos, 2002). Among them, *Aedes aegypti* is of
49 particular importance because of its wide distribution and its capacity to transmit Yellow fever,
50 Dengue, Zika and Chikungunya viruses (Brown et al., 2014). These arboviruses are now re-emerging
51 worldwide following the expansion of mosquitoes' distribution area as a consequence of global
52 warming, global transportation network and land perturbations (Kraemer et al., 2015). Although
53 efforts are invested in improving vaccine-based prevention strategies (Carvalho & Long, 2021; Garg
54 et al., 2020; Silva et al., 2018), vector control remains the cornerstone of arboviral diseases control.
55 However, decades of insecticide usage have led to the selection and spread of insecticide resistance
56 in this mosquito species, affecting all public health insecticides, including the most-used pyrethroids
57 (Moyes et al., 2017). High pyrethroid resistance has been shown to reduce vector control efficacy
58 (Dusfour et al., 2011; Marcombe, Carron, et al., 2009; Marcombe et al., 2011; Valle et al., 2019).
59 Though greener vector control strategies are being developed, insecticides will likely remain a key
60 component of integrated vector control in high transmission areas for the next decades (Achee et al.,
61 2019). In this concern, identifying the genetic factors underlying resistance is crucial for tracking
62 resistance alleles in the field and making a better use of the few authorised public health insecticides

through resistance management actions (Cattel et al., 2020; Corbel & N'Guessan, 2013; Dusfour et al., 2019).

In mosquitoes, resistance to chemical insecticides is mainly caused by genetic changes decreasing the affinity of the insecticide for its target (target-site resistance), decreasing its penetration (cuticular resistance), or increasing its detoxification through complex biochemical pathways (metabolic resistance) (Li et al., 2007). Pyrethroid insecticides target the neuronal voltage-gated sodium channel (*VGSC* gene), and the selection of *knockdown resistance* (*kdr*) mutations affecting this protein can lead to resistance. Multiple *kdr* mutations, often combined as haplotypes, have been identified in *Ae. aegypti* with the following ones shown to play a key role in pyrethroid resistance: Val410Leu, Leu982Trp, Ser989Pro, Val1016Gly/Ile and Phe1534Cys (Brengues et al., 2003; Haddi et al., 2017; Hirata et al., 2014; Kasai et al., 2022; Saavedra-Rodriguez et al., 2007; Smith et al., 2016; Yanola et al., 2011). Today, these mutations can be tracked in the field using PCR-based diagnostic assays or mass sequencing approaches, providing essential information for resistance management programmes (Melo Costa et al., 2020).

Conversely, the genetic bases of metabolic resistance are far less understood, though it often accounts for a significant part of the phenotype (David et al., 2013). Indeed, the complexity and redundancy of xenobiotic biodegradation pathways often lead to multigenic adaptations that can differ according to the nature and intensity of the selection pressure together with the demographic and ecological context (Feyereisen et al., 2015; Li et al., 2007). Metabolic resistance to pyrethroids usually results from an increased activity of detoxification enzymes such as cytochrome P450 monooxygenases (P450s or *CYPs* for genes), glutathione S-transferases (GSTs) carboxy/cholinesterases (CCEs) and UDP-glycosyl-transferases (UDPGTs) (David et al., 2013; Hemingway et al., 2004; Smith et al., 2016). At the genetic level, this can result from the selection of enzyme variants showing a higher insecticide metabolism rate, or their overexpression through cis- or trans- regulation. Genomic duplications can also contribute to overexpression, and duplications affecting detoxification genes appear frequently associated with insecticide resistance in mosquitoes (Cattel et al., 2020, 2021; Faucon et al., 2015; Weetman et al., 2018).

In addition to the genetic complexity of metabolic resistance alleles, their frequent co-occurrence with other resistance mechanisms in natural mosquito populations makes them difficult to characterise. This is the case in French Guiana, where the use of the pyrethroid deltamethrin for decades has led to the selection of highly resistant *Ae. aegypti* populations combining metabolic resistance alleles and multiple *kdr* mutations such as Val410Leu, Val1016Ile or Phe1534Cys (Dusfour et al., 2015; Haddi et al., 2017). Although the over-expression of several detoxification enzymes was supported by transcriptomics and proteomics (Dusfour et al., 2015; Epelboin et al., 2021; Faucon et

97 al., 2017), detoxification enzymes most contributing to deltamethrin resistance and the underlying
98 genetic events remain to be identified. A recent study using a composite population from French
99 Guiana identified copy number variations (CNV) as a probable cause of overexpression of
100 detoxification enzymes in this region (Cattel et al., 2020). One particular locus spanning multiple
101 P450s showed some evidence of duplication, however the high frequency of *kdr* mutations
102 decreased the association power while the exon-sequencing approach did not allow resolving the
103 genomic architecture of the duplicated locus.

104 In this context, the present study aimed at confirming the contribution of this duplication in the
105 resistance of *Ae. aegypti* to deltamethrin and at deciphering its genomic architecture. Two isofemale
106 lines originating from French Guiana and showing contrasted pyrethroid resistance levels were used;
107 both lacking two major *kdr* mutations Val1016Ile and Val410Leu occurring in South America
108 (Epelboin et al., 2021). Controlled crosses were used to remove the Phe1534Cys *kdr* mutation from
109 the resistant line, which retained a P450-mediated resistance phenotype. Then, RNA-seq and whole
110 genome pool-seq confirmed the presence of a ~200 Kb genomic duplication enhancing the
111 expression of a cluster of multiple P450 genes in the resistant line. The genomic architecture of the
112 duplicated loci was elucidated through long read sequencing, providing clues about its evolutionary
113 origin. Association studies, experimental evolution and reverse genetic were then used to investigate
114 the contribution of this duplicated allele in deltamethrin resistance.

115

116 # Results

117

118 *Deltamethrin resistance is associated with P450 activity*

119 Individual crossings within the resistant line IR03 allowed producing the IR0F line deprived of *kdr*
120 mutations majorly associated with pyrethroid resistance in South America (*i.e.* Val410Leu,
121 Val1016Ile, Phe1534Cys). However, our attempts to remove the only *kdr* mutation remaining,
122 Ile1011Met were not successful (see below). Comparative deltamethrin bioassays showed that the
123 IR0F line remained highly resistant to deltamethrin with 44% mortality, as compared to the IR13 line
124 and the fully susceptible strain Bora-Bora showing 95% and 100% mortality respectively (**Table 1**).
125 Mortality levels remains similar between the IR03 line and the IR0F line suggesting that the removal
126 of the Phe1534Cys *kdr* mutation did not affect the resistance phenotype, or was compensated by the
127 retaining of the Ile1011Met *kdr* mutation.

128
129

130 **Table 1. Origin, resistance status and *kdr* mutations frequencies of the studied lines**

Line	Origin, type	Deltamethrin mortality[1]	Resistance status	f(410Leu) [2,3]	f(1016Ile) [2,3]	f(1534Cys) [2,3]	f(1011Met) [3]
Bora-Bora	Fr. Polynesia, Lab	100	Susceptible	0	0	0	0
IR13	Fr. Guiana, isofemale	95 (91-99)	Low resistance	0	0	0.26	0
IR03	Fr. Guiana, isofemale	43 (26-60)	Resistant	0	0	0.26	0.33
IR0F	IR03 cross	44 (34-54)	Resistant	0	0	0	0.50

131 [1] Mortality rates (mean ±SD) previously obtained on 3 days-old females using 0.05% deltamethrin for 40 min (N=10).
132 [2] *Kdr* mutation frequencies estimated by qPCR genotyping (N=30).
133 [3] *Kdr* mutation frequencies estimated from pool-seq data.
134

135 In order to test the involvement of P450s in the pyrethroid resistance phenotype, we sequentially
136 exposed adult mosquitoes to the P450 inhibitor piperonyl butoxide (PBO) and to deltamethrin. Such
137 PBO pre-exposure did not significantly affect survival in the susceptible IR13 line, but increased
138 mortality by 20% in the IR0F line (Wilcoxon test P value = 0.009), supporting the contribution of
139 P450-mediated detoxification in the resistance of the IR0F line (**Figure 1**).

140

141 *The resistance phenotype is autosomal and semi-dominant*

142 Comparative deltamethrin bioassays performed on F1 and F2 males and females from '*Bora-Bora x*
143 *IR0F'* reciprocal crosses did not support any significant bias affecting the transmission of resistance
144 alleles (**Supplementary file 1**). The mortality levels in F1 upon deltamethrin exposure were
145 intermediate to those of the parental lines for both males and females in both crosses, indicating the
146 absence of a maternal effect. Intermediate mortality levels were again observed in F2, suggesting the
147 lack of a sex transmission bias. Overall, the resistance phenotype behaved as semi-dominant.

148

149 *The resistance phenotype is associated with a duplication affecting multiple P450s*

150 RNA-seq was used to identify differentially transcribed genes between the two resistant lines (IR03
151 and IR0F), and the two susceptible lines (IR13 and Bora-Bora). Among the 11078 genes detected, 84
152 genes showed a significant and consistent differential transcription level in the four '*resistant Vs*
153 *susceptible'* pairwise comparisons (see methods, expression fold change ≥ 1.5 and adjusted P value ≤
154 0.0005). The 39 genes under-transcribed in resistant lines did not include any gene belonging to any
155 family known to be associated with insecticide resistance. Conversely, the 45 genes over-transcribed
156 in resistant lines included 8 genes belonging to gene families associated with metabolic resistance
157 (**Figure 2** and **Supplementary file 2**). These included five P450s (*CYP6BB2* AAEL014893, *CYP6-like*
158 AAEL026852, *CYP6-like* AAEL017061, *CYP6P12* AAEL014891 and *CYP9F-like* AAEL028635). The four
159 *CYP6* genes showed mean fold changes up to 4.0 folds and belong to a cluster of five consecutive

160 *CYP6* genes located at ~271 Mb on chromosome 1. Among them, *CYP6P12* (AAEL014891) was
161 annotated as a single accession in the reference genome while both protein sequence and RNA-seq
162 data support the presence of two genes hereafter referred to as *CYP6P12v1* and *CYP6P12v2* when
163 appropriate.

164 Whole genome Pool-seq data were then used to identify genes affected by copy number variations in
165 association with resistance base on their normalised exonic coverage. This analysis identified 43
166 genes showing congruent copy number variations between resistant and susceptible lines (FC ≥ 1.5 in
167 all *'resistant Vs susceptible'* pairwise comparisons). The 22 genes showing an elevated copy number
168 in resistant lines included seven P450s. One of them (AAEL009018) was located at ~58.8 Mb on
169 chromosome 1 and was not detected as over-transcribed from RNA-seq. The six others were located
170 at ~271 Mb on chromosome 1 and included the five *CYP6s* found over-transcribed in resistant lines
171 (see above) and another *CYP6* (*CYP6CC1*) from the same gene cluster that was filtered out from RNA-
172 seq analysis due to a very low transcription level (**Figure 2** and **Supplementary file 2**). A closer look at
173 the genomic coverage at this locus revealed a ~2 folds increased coverage affecting a region of ~200
174 Kb spanning the entire *CYP6* cluster. Such duplication was observed in both resistant lines (IR03 and
175 IR0F). Altogether, these genomic data suggest that the deltamethrin resistance phenotype observed
176 in the IR03 and IR0F lines is associated with a large duplication on chromosome 1 affecting the
177 transcription level of six clustered *CYP6* genes.

178 Whole genome pool-seq data confirmed the absence of the major Val410Leu, Val1016Ile and
179 Phe1534Cys *kdr* mutations in the resistant IR0F line, while another *kdr* mutation (Ile1011Met) was
180 identified at an exact 0.5 frequency (141/282 reads supporting the 1011Met allele). Indeed, both
181 short read and long read data revealed that this Ile1011Met mutation is part of an imperfect
182 genomic duplication covering the 21 last exons of the *VGSC* gene AAEL023266 (**Supplementary file**
183 **3**), the partial copy bearing the wild type (Ile) allele and the full-length copy bearing the resistant
184 (Met) allele (Martins et al., 2013). A 0.5 frequency thus indicates that the Ile-Met/Ile-Met genotype is
185 fixed in the IR0F line. As expected from an imperfect duplication, RNA-seq data support the sole
186 expression of the Met allele in the IR0F line, leading to a Met/Met phenotype.

187

188 *Genomic architecture of the duplication*

189 The genomic structure of the duplicated region previously identified on chromosome 1 from short
190 read data was further investigated in light of long reads data obtained from the IR13 susceptible line
191 and the IR0F resistant line. This revealed the presence of a 220.4 Kb duplication in the IR0F line, with
192 the two tandem repeats separated by a 6 Kb insertion (**Figure 3**). The right breakpoint of the

193 duplication (RB) was found ~50 Kb right to *CYP6CC1* at position 271,472,082 bp, and the left
194 breakpoint (LB) ~77 Kb left to *CYP6BB2* at 271,251,705 bp. These breakpoints were supported by split
195 reads from both long and short read data (**Supplementary file 4**). The duplication is flanked by two
196 distinct transposons, each having its own terminal inverted repeats (TIR): a 2.4 Kb PiggyBac-like
197 transposon on the right (PYL), and 9 Kb hAT-related transposon on the left (hAT-CYP6). These
198 transposons are described in more detail in **Supplementary file 5**. The central sequence joining the
199 tandem copies is chimeric, with 60 bp from the left end of PYL transposon followed by 6001 bp from
200 the right end of the hAT transposon. This duplication is absent from the IR13 susceptible line (no
201 read joining RB and LB sequences and no PYL transposon sequence, neither full nor partial at RB).
202 However, the hAT-CYP6 transposon was identified at the LB in one IR13 haplotype, much like in the
203 IR0F line, while a second haplotype was devoid of hAT insertion, much like the reference genome. An
204 excess of tri-allelic SNPs is expected within the duplication if the two copies have diverged. To
205 investigate this, Pool-seq data from the IR0F line were searched for such tri-allelic SNPs within the
206 duplication and 100 Kb upward and downward. Loci were considered as tri-allelic if they carried two
207 distinct variant alleles at the same position with a minimum allele frequency > 20%. Among the 1401
208 substitutions sites identified within the duplication, five were tri-allelic. No such tri-allelic variant was
209 identified among the 1334 substitutions identified in flanking regions, representing a slight but
210 significant enrichment in the duplicated region (Fisher test p value = 0.035). These tri-allelic sites
211 were all located within a 11.2 Kb intergenic region between the two *CYP6-like* genes AAEL017061 and
212 AAEL014891v1.

213

214 *The P450 duplication is associated with deltamethrin survival*

215 The association of the P450 duplication and the *kdr* Ile1011Met mutation with deltamethrin survival
216 were investigated in F2 individuals obtained from both 'Bora-Bora x IR0F' reciprocal crosses. F2
217 females were then segregated with a high dose of deltamethrin (85.5% mortality) before quantifying
218 *CYP6BB2* gene copy number and the frequency of the 1011Met *kdr* allele using ddPCR (**Figure 4**). As
219 expected in the presence of a fixed duplication, a 2-fold increase of *CYP6BB2* copy number was
220 observed in the IR0F line (4.31 ± 0.21 copies) as compared to Bora-Bora line (2.07 ± 0.10 copies)
221 while F1 individuals showed an intermediate copy number (3.58 ± 0.14 copies). In deltamethrin
222 segregated F2 individuals, *CYP6BB2* copy number was higher in survivors than in dead individuals
223 (4.00 ± 0.16 copies versus 3.31 ± 0.15 copies) supporting a genetic linkage between the P450
224 duplication and resistance. Resistance was also linked to the *kdr* mutation Ile1011Met on
225 chromosome 3. In line with an heterogenous *kdr* duplication, the frequency of the Met allele was
226 close to 0.5 in the IR0F resistant line and close to 0.33 in F1 individuals. In deltamethrin-segregated

227 F2 individuals, the Met allele frequency was higher in survivors than in dead individuals (0.41 ± 0.02
228 versus 0.30 ± 0.02).

229

230 *Multiple P450s carried by the duplication may contribute to deltamethrin survival*

231 The relative importance of the P450s carried by the duplication in deltamethrin survival was then
232 examined by RNA interference. Direct dsRNA injections in adult females of the IR0F line were used to
233 specifically knock down the five *CYP6* genes showing sufficient expression to be detected by RNA-seq
234 (*CYP6BB2*, *CYP6-like* AAEL026582, *CYP6-like* AAEL017061, *CYP6P12v1* and *CYP6P12v2*). Such
235 approach allowed reaching an acceptable silencing specificity and a moderate silencing efficiency
236 (from 42.2% for AAEL017061 to 69.7% for AAEL026582). Comparative deltamethrin bioassays
237 performed on dsCYP6-injected mosquitoes and dsGFP-injected controls suggested that the two first
238 CYP gene of the duplicated cluster (*CYP6BB2* and *CYP6-like* AAEL026582) contribute to deltamethrin
239 survival (see methods and results in **Supplementary file 6**). However, data generated across multiple
240 injection experiments were not fully conclusive because a high mortality was frequently observed in
241 dsGFP-injected controls and because the increased mortality observed in dsCYP-injected mosquitoes
242 were relatively low probably due to the moderate silencing efficiency and the presence of the *kdr*
243 1011Met allele in the IR0F line.

244

245 *The duplication is hardly retained by selection in presence of the 1011Met kdr allele*

246 The co-occurence of the P450 duplication and the Ile1011Met *kdr* mutation in the IR0F resistant line
247 was taken as an opportunity to compare their responses to deltamethrin selection. Four independent
248 lines obtained from 'Bora-Bora x IR0F' F3 offspring and representing two replicated selection regimes
249 (selected lines: SelA and SelB, non-selected lines: NSA and NSB) were compared for their resistance
250 level, *CYP6BB2* copy number and *kdr* 1011Met allele frequency (**Figure 5**). An increase of
251 deltamethrin resistance was observed for both Sel lines, with mortality dropping from ~80% in F4 to
252 less than 20% in F9. Relaxing deltamethrin selection for three successive generations (F9 to F11) lead
253 to an increased mortality in both Sel lines, suggesting that the resistance phenotype is costly. Though
254 subjected to sampling effects, ddPCR data showed that the *kdr* 1011Met allele was rapidly selected
255 by deltamethrin. Its frequency was close to 0.5 in F9 of both Sel lines, supporting the near fixation of
256 the Ile-Met duplicated allele. Such increased frequency was not seen in NS lines where Met allele
257 frequency decreased to less than 10% in one line and fluctuated under 0.25 in the other line. No such
258 strong response to selection was observed for the P450 duplication, with *CYP6BB2* copy number
259 showing a gradual decrease through generations in both Sel and NS lines. However, *CYP6BB2* mean

260 copy number were significantly higher in Sel lines than in NS lines across generations, supporting a
261 higher retention rate of the duplicated allele upon deltamethrin selection (Linear Mixed Effect
262 Model, p value = 0.0088).

263

264 Discussion

265 In line with their high probability of occurrence, genomic duplications have been shown to frequently
266 contribute to short-term adaptation in various organisms (Kondrashov, 2012). In arthropods facing
267 strong selection pressures from insecticides, duplications are known to be adaptive via two distinct
268 mechanisms (Bass & Field, 2011). First, heterogeneous duplications affecting key insecticide target
269 genes and tethering both susceptible and resistant alleles have been associated with a reduction of
270 fitness costs (Labbe et al., 2007). Second, duplications of detoxification genes can contribute
271 quantitatively to their over-expression, leading to resistance through increased insecticide
272 metabolism (Faucon et al., 2015; Weetman et al., 2018). As opposed to target-site resistance
273 mutations that can be easily tracked by PCR in natural populations, the paucity of DNA markers
274 underlying metabolic resistance hinders their tracking in the field. In this concern, identifying gene
275 duplications associated with metabolic resistance can provide new tools to monitor the dynamics of
276 resistance alleles (Cattel et al., 2021).

277

278 *A genomic duplication affects a cluster of P450s previously associated with resistance*

279 The present study confirmed the occurrence of a large genomic duplication affecting a cluster of six
280 P450s from the *CYP6* family in *Ae. aegypti* populations from French Guiana. The presence of such a
281 duplication was previously suspected though the structure of the duplicated loci could not be
282 resolved from targeted-sequencing data (Faucon et al., 2015). The association of this P450
283 duplication with deltamethrin resistance was supported by controlled crosses, although the presence
284 of other resistance alleles limited the association power (Cattel et al., 2020). A duplication
285 encompassing the *CYP6BB2* gene was also associated with pyrethroid resistance in Lao PDR
286 (Marcombe et al., 2019), suggesting a wider geographic distribution. Though gene duplication was
287 not looked for, the over-transcription of CYP6 genes from this cluster (e.g. *CYP6BB2*, *CYP6P12* and
288 *CYP6CC1*) was frequently associated with pyrethroid resistance worldwide (Bariami et al., 2012;
289 Dusfour et al., 2015; Goindin et al., 2017; Kasai et al., 2014; Marcombe, Poupardin, et al., 2009;
290 Moyes et al., 2017; Reid et al., 2014; Saavedra-Rodriguez et al., 2012; Seixas et al., 2017). These
291 genes were also found under directional selection in association with pyrethroid survival in a

292 Mexican resistant line from whole exome SNP data (Saavedra-Rodriguez et al., 2021). In addition,
293 *CYP6BB2* was also shown capable of metabolising the pyrethroid permethrin (Kasai et al., 2014). By
294 comparing its copy number and transcriptional level across different lines, Faucon et al. (2017)
295 suggested that both transcriptional regulation and genomic duplication contribute to its over-
296 expression in South America. Interestingly, this gene also responded to selection with the
297 neonicotinoid imidacloprid, suggesting that P450s from this cluster can be selected by and
298 metabolise other insecticides (Riaz et al., 2013; Zoh et al., 2021).

299 Our attempt to isolate this P450 duplication from other resistance alleles occurring in French Guiana
300 was partially successful. Indeed, both isofemale lines were naturally deprived from the major
301 Val1016Iso and Val410Leu *kdr* mutations, and controlled crosses allowed removing the Phe1534Cys
302 mutation. However, the resulting IR0F resistant line carrying the P450 duplication still carried the
303 Ile1011Met *kdr* mutation as a fixed heterogenous duplication (Ile-Met/Ile-Met genotype, Met/Met
304 phenotype). Nevertheless, the use of the P450 inhibitor PBO showed that the resistance phenotype
305 was still associated with P450-mediated metabolism. Considering that four of the five P450s over-
306 transcribed in resistant lines belong to the duplicated loci, their contribution to the resistance
307 phenotype is likely. Studying the mode of transmission of resistance did not allow evidencing any
308 significant maternal effect or sexual transmission bias potentially associated with resistance. In line
309 with this, this P450 duplication is located outside of a 210 Mb region of chromosome 1 showing a low
310 recombination rate and a high genetic differentiation between *Ae. aegypti* males and females
311 (Fontaine et al., 2017).

312

313 *The architecture of the P450 duplication suggests a recent ectopic recombination event*

314 The presence of two distinct transposons at the duplication breakpoints that they have played an
315 active role in the generation of this genomic event. Transposon-mediated duplication often arises
316 from ectopic recombination between two homologous transposon copies inserted in the same
317 orientation at distinct positions of a same chromosome (Baker et al., 1996). However, such an event
318 would leave a single full-length transposon copy between the two duplicated genomic regions with
319 no transposon at other breakpoints (Remnant et al., 2013). Here, a more complex scenario must
320 have taken place because two distinct transposons are flanking the duplication, and because the
321 sequence joining the two copies is chimeric. A possible scenario involves independent insertion of
322 the two distinct transposons, then transposition of the hAT into the PiggyBac-like transposon
323 followed by a deletion event, and finally an ectopic homologous recombination event between the
324 two duplicated hAT sequences (**Supplementary File 7**). One transposon involved is related to the hAT

325 superfamily while the other one is distantly related to PiggyBac (see **Supplementary file 5** for more
326 details), both being cut and paste elements having multiple copies and being active in the *Ae. aegypti*
327 genome (Nene et al., 2007). The divergence of the two tandem copies was supported by the
328 identification of a few tri-allelic substitution sites within the duplicated region. Though the frequency
329 of such tri-allelic sites is likely underestimated (*i.e.* reverting mutations to the wildtype allele not
330 detected as tri-allelic), such low divergence supports the recent age of this duplication event.

331

332 *The P450 duplication is associated with deltamethrin survival but its adaptive value may be*
333 *balanced by its fitness cost*

334 The association study confirmed the association of the P450 duplication with deltamethrin survival
335 together with the Ile1011Met *kdr* mutation. As the *VGSC* gene carrying *kdr* mutations is located on
336 chromosome 3, a genetic linkage between these two loci is excluded. The association of the P450
337 duplication in F2, following limited recombination events, implies a resistance locus located on
338 chromosome 1, either the P450 duplication itself or another genetically linked locus. However, no
339 other known resistance gene was identified in this genomic region in the present study. The
340 association of the Ile1011Met *kdr* mutation with deltamethrin survival was expected. Indeed,
341 although less efficient than other *kdr* mutations (Brito et al., 2018), there is evidence that this
342 mutation confers some resistance to deltamethrin in the field (Brengues et al., 2003; Martins et al.,
343 2009). As previously suggested, we identified that this *kdr* mutation is part of a heterogenous
344 duplication (Martins et al., 2013). Our RNA-seq data supported the sole expression of the Met allele
345 in the IR0F resistant line, suggesting that the wild type Ile allele is carried by a pseudo gene.

346 The relative importance of the different *CYP6* genes carried by the P450 duplication in deltamethrin
347 survival was investigated through RNA interference. Despite a limited statistical power, likely due to
348 the presence of the *kdr* Ile1011Met resistance allele and moderate knock down efficiencies, these
349 data suggest that at least two *CYP6* genes (*CYP6BB2* and AAEL026582) carried by the duplication may
350 contribute to deltamethrin survival.

351 Experimental evolution confirmed the strong positive response of the *kdr* 1011Met allele to selection
352 with a high dose of deltamethrin. Such experiment also evidenced a gradual decrease of this allele in
353 both non-selected lines, supporting a fitness costs in absence of insecticide as previously shown for
354 other *kdr* mutations (Rigby et al., 2020; Uemura et al., 2023). Indeed, the co-existence of the Met
355 allele carried by the full length *VGSC* gene and the duplicated Ile allele carried by a pseudogene
356 would not confer a fitness cost reduction as seen for the Ace-1 locus in *Culex pipiens sp.* and
357 *Anopheles gambiae* where both alleles contribute to the phenotype (Djogbenou et al., 2009; Labbe

358 et al., 2007). In this regard, further investigating the evolutionary origin and dynamics of this *kdr*
359 duplication in relation to insecticide selection pressure deserves further attention.

360 The association of the P450 duplication with resistance was less clear. A gradual decrease of *CYP6BB2*
361 copy number was observed in both selected and non-selected lines, even though such decay was
362 slower in the selected lines. Such result may indicate the presence of a significant fitness cost
363 associated with this large genomic duplication, that is not compensated by its adaptive value in our
364 laboratory conditions. Indeed, genomic duplications can be detrimental for various reasons (Schrider
365 et al., 2013): first, gene duplications can alter the gene dosage balance which can lead to metabolic
366 cost. Second, genomic duplications allow the accumulation of deleterious mutations that are less
367 cleared off by background selection because of the functional redundancy of duplicated copies.
368 Third, large duplications can impair recombination locally. In the present case, a low recombination
369 rate at this locus between the Bora-Bora line (well adapted to laboratory conditions) and the IR0F
370 line (less fitted to our laboratory conditions) may have impaired the selection of the P450 duplication
371 and favoured the selection of the *kdr* 1011Met allele. Finally, considering the fitness costs associated
372 with this *kdr* mutation, its additive cost with the P450 duplication may have prevented their
373 concomitant selection with the use of high insecticide dose favouring the selection of the former.
374 Such fitness-cost balance at two distinct loci may reflect the complex interactions occurring between
375 resistance alleles *in natura*, leading to distinct adaptive trajectories depending on selection pressures
376 and demographic effects.

377

378 *Conclusions*

379 Following previous work, the present study supports the contribution of this P450 duplication in
380 pyrethroid resistance. However, deciphering its adaptive value *versus* other resistance alleles and its
381 dynamics in natural mosquito populations deserves further work. The relative importance of the
382 different *CYP6* genes carried by this duplication in resistance to pyrethroids (and possibly to other
383 insecticides) also deserves further validation. Despite this incomplete picture, the nature of the
384 P450s affected by this large genomic duplication and their frequent association with insecticide
385 resistance call for further studying its evolutionary origin and dynamics in response to xenobiotics. In
386 this context, though the flanking of the duplication by repeated transposable elements prevented
387 the design of a specific PCR diagnostic assay targeting the breakpoints, the dual-colour quantitative
388 TaqMan ddPCR assay we developed (see **Supplementary file 8**) represents a good alternative to track
389 this resistance allele in natural mosquito populations.

390

391 # Methods

392 *Mosquitoes*

393 The *Ae. aegypti* laboratory strain Bora-Bora, fully susceptible to insecticides was used as reference in
394 the present study. The isofemale lines used in the present study were derived from a field population
395 collected in 2015 in the Ile Royale (IR) island (5.287° N; 52.590° W) off the coast of French Guiana as
396 described in Epelboin et al. (2021). Among the isofemale lines isolated from this population, the lines
397 IR13 and IR03 showed contrasted pyrethroid resistance levels with the IR03 line being highly
398 resistant and the IR13 line being susceptible. Both lines were shown to lack the two major voltage-
399 gated sodium channel *kdr* mutations occurring in this geographical area (Val410Leu and Val1016Ile),
400 yet both carried the Phe1534Cys mutation at a moderate frequency (Epelboin et al., 2021). The
401 proteomic profiling of these lines identified multiple cytochrome P450s enriched in the IR03 resistant
402 line as compared to a susceptible line, supporting the presence of metabolic resistance alleles
403 (Epelboin et al., 2021). All mosquito lines were maintained under standard laboratory conditions (27
404 ± 2°C, 70 ± 10 % relative humidity, light/dark cycle 14:10h) and large population size to limit drift
405 effects (N>1000). Larvae were reared in tap water and fed with hay pellets. Adults were maintained
406 in mesh cages and fed with a 10% honey solution. Blood feedings were performed on mice.

407

408 *Removal of the Phe1534Cys mutation from the IR03 line*

409 In an attempt to isolate metabolic resistance alleles, inter-crosses assisted by genotyping were
410 performed on the IR03 resistant line to create the IR0F line depleted from the Phe1534Cys *kdr*
411 mutation. A total of 245 IR03 couples were individualised at the pupal stage in eppendorf tubes
412 placed in plastic cups covered by a nylon mesh and allowed to emerge and reproduce. The
413 Phe1534Cys Kdr mutation was first searched for from male exuvia for all couples and then from
414 female exuvia of the 58 couples from which males were negatives for the 1534Cys allele. Genotyping
415 was performed on qPCR using the High Resolution Melt Curve Analysis method as described in
416 Saavedra-Rodriguez et al. (2007). The six couples in which both parents were homozygous wild type
417 (Phe-Phe) were transferred to a mesh cage, blood fed and allowed to lay eggs. The absence of the
418 1534Cys allele in the offspring was confirmed by genotyping 40 individuals of both sexes. Adults were
419 then exposed to 0.05% deltamethrin and survivors were allowed to freely reproduce to generate the
420 IR0F resistant line. The IR0F line was then maintained in standard insectary conditions under
421 moderate deltamethrin selection pressure (*i.e.* 50% mortality every two generations).

422

423 *Deltamethrin bioassays*

424 All bioassays were performed by exposing replicates of 20-25 three days-old non-blood-fed adults to
425 deltamethrin impregnated filter papers following the standard WHO procedure, with mortality being
426 recorded 24h after insecticide exposure (WHO, 2022). Different doses and exposure times were used
427 according to the nature of the mosquito tested (susceptibility status, sex, use of enzymatic inhibitor)
428 in order to maximise the mortality variations observed. Bioassay assessing the resistance level of the
429 different lines was performed on females using 10 replicates per line and a dose of 0.05%
430 deltamethrin for 40 min. The involvement of P450s in the resistance phenotype was assessed by
431 comparing deltamethrin mortality of females exposed or not to filter papers impregnated with 4%
432 piperonyl butoxide (PBO) for 1h prior to deltamethrin bioassay. This bioassay was performed on 5
433 replicates for each condition and a dose of 0.03% deltamethrin for 30 min. In order to investigate the
434 mode of inheritance of resistance, comparative bioassays were performed on males and females
435 obtained from the susceptible Bora-Bora line and the resistant IR0F line together with F1 and F2
436 individuals obtained from their reciprocal crosses (see below). Deltamethrin exposure conditions
437 were 0.03% deltamethrin for 30 min for females and 0.015% deltamethrin for 25 min for the males
438 to account for their inherent lower insecticide tolerance. Bioassays used for monitoring the
439 resistance level of the selected and non-selected lines during experimental evolution were
440 performed on 5 to 7 replicates per line per generation using a dose of 0.03% deltamethrin for 1h.

441

442 *Controlled cross and association studies*

443 In order to investigate the mode of inheritance of resistance, reciprocal crosses between the fully
444 susceptible Bora-Bora line and the resistant IR0F line were performed (cross A: 'Bora-Bora females x
445 IR0F males' and cross B: 'IR0F females x Bora-Bora males'). Crosses were performed with 200 virgin
446 females and males of each line. The susceptibility of F1 and F2 males and females from each cross
447 were then compared using deltamethrin bioassays as described above. The association of the P450
448 duplication with deltamethrin survival was studied in F2 females obtained from both reciprocal
449 crosses. Females were segregated with 0.03% deltamethrin for 1h leading to 88.5% mortality after a
450 24h recovery time. Dead and alive females were sampled and stored at -20°C until molecular
451 analyses. The response of the P450 duplication and the Ile1011Met *kdr* mutation were further
452 studied across multiple generations using experimental selection. F3 eggs obtained from the two
453 reciprocal crosses A and B were pooled in equal quantity and then randomly split in 4 lines: the first
454 two lines (NSA and NSB) were maintained without insecticide selection, while the two other lines

455 (SelA and SelB) were selected with deltamethrin. This duplicated line setup was used in order to
456 control for genetic drift that may occur across generations. Deltamethrin mass selection was
457 performed prior mating on both virgin males and virgin females (N>1000 for each line) at generations
458 F4, F6, F8, F12 and F13. A constant dose of deltamethrin was used through the selection process
459 leading to ~70% mortality in each sex at generation F3 (females: 0.03% for 1h; males: 0.015% for 30
460 min). The resistance level of each line was monitored at generations F5, F9, F12, F13 and F14 on
461 females prior to insecticide selection using standard bioassays (see above). Unexposed adult females
462 from each line were sampled at the same generations and stored at -20°C until molecular analysis.

463

464 *RNA-sequencing*

465 Gene transcription levels were compared across the four lines (Bora-Bora, IR13, IR03 and IR0F) using
466 RNA-seq. For each line, four RNA-seq libraries were prepared from distinct batches of 25 calibrated
467 three-day-old non-blood-fed females not exposed to insecticide. Total RNA was extracted using
468 TRIzol (Thermo Fisher Scientific) following manufacturer's instructions. RNA samples were then
469 treated with RNase-free DNase set (Qiagen) to remove gDNA contamination, purified on RNeasy mini
470 columns (Qiagen) and QC checked using Qubit (Thermo Fisher Scientific) and bioanalyzer (Agilent).
471 RNA-seq libraries were prepared from 500 ng total RNA using the NEBNext® Ultra™ II directional RNA
472 library Prep Kit for Illumina (New England Biolabs) following manufacturer's instructions. Briefly,
473 mRNAs were captured using oligodT magnetic beads and fragmented before being reverse
474 transcribed using random primers. Double-stranded cDNAs were synthesised, end-repaired, and
475 adaptors were incorporated at both ends. Libraries were then amplified by PCR for 10 cycles and
476 purified before QC check using Qubit and Bioanalyzer. Libraries were then sequenced in multiplex as
477 single 75 bp reads using a NextSeq500 sequencer (Illumina). An average of 51.4 M reads was
478 generated per library. After unplexing and removing adaptors, sequenced reads from each library
479 were loaded into Strand NGS V3.2 (Strand Life Science) and mapped to the latest *Ae. aegypti* genome
480 assembly (Aaeg L5) using the following parameters: min identity = 90%, max gaps = 5%, min aligned
481 read length = 25, ignore reads with > 5 matches, 3′ end read trimming if quality < 20, mismatch
482 penalty = 4, gap opening penalty = 6, gap extension penalty = 1. Mapped reads were then filtered
483 based on their quality and alignment score as follows: mean read quality > 25, max N allowed per
484 read = 5, alignment score ≥ 90, mapping quality ≥ 120, no multiple match allowed, read length ≥ 35.
485 These filtering steps allowed retaining ~75% of reads. Quantification of transcription levels was
486 performed on the 13614 protein-coding genes using the DESeq2 method with 1000 iterations
487 (Anders & Huber, 2010, https://bioconductor.org/packages/release/bioc/html/DESeq2.html). Only
488 the 11449 genes showing a normalised expression level ≥ 0.5 (~0.05 RPKM) in all replicates for all

489 lines were retained for further analysis. Differential gene transcription levels between each line
490 across all replicates were then computed using a one-way ANOVA followed by a Tukey post hoc test
491 and p values were corrected using the Benjamini and Hochberg multiple testing correction
492 (Benjamini & Hochberg, 1995). Genes showing a transcription variation ≥ 1.5 fold (in either direction)
493 and an adjusted p value ≤ 0.0005 in the four pairwise comparisons between resistant and susceptible
494 lines (*i.e.* IR03 Vs Bora-Bora, IR03 Vs IR13, IR0F Vs Bora-Bora and IR0F Vs IR13), were considered
495 differentially transcribed in association with deltamethrin resistance.

496

497 *Whole genome Pool-seq and CNV analysis*

498 The genome of the four lines were compared using whole genome pool-seq. For each line, genomic
499 DNA was extracted from two batches of 50 adult females using the PureGene Core Kit A (Qiagen) and
500 the two gDNA extracts were then pooled in equal proportion into a single sequencing library. Whole
501 genome sequencing was performed from 200 ng gDNA. Sequencing libraries were prepared
502 according to the TruSeq DNA Nano Reference guide for Illumina Paired-end Indexed sequencing
503 (version oct. 2017) with an insert size of 550 bp. Sequencing was performed on a NextSeq 550
504 (Illumina) as 150 bp paired-reads. Sequencing depth was adjusted to reach an average coverage ≥
505 80X leading to the sequencing of ~713 M reads per library. Reads obtained from each line were
506 loaded into Strand NGS V3.2 and mapped to *Ae. aegypti* genome (Aaeg L5) using the following
507 parameters: min identity = 90%, max gaps = 5%, min aligned read length = 25, ignore reads with > 5
508 matches, 3 end read trimming if quality < 15, mismatch penalty = 4, gap opening penalty = 6, gap
509 extension penalty = 1. Mapped reads were then filtered based on their quality and alignment score
510 as follows: mean read quality > 25, max N allowed per read = 5, alignment score ≥ 90, mapping
511 quality ≥ 60, no multiple match allowed, read length ≥ 100. Finally, interchromosomal split reads and
512 PCR duplicates were removed. These filtering steps allowed retaining ~53% of reads. In order to
513 focus on duplication impacting protein expression, gene copy number variation (CNV) analysis was
514 performed on exons of all protein-coding genes. For each gene, raw coverages were obtained by
515 dividing the number of reads mapped to all (non-overlapping) exons by total exon length. Normalised
516 gene coverages were then obtained by dividing raw gene coverages by the total number of reads
517 passing mapping and quality filters from each sequenced library. In order to limit false positives in
518 low coverage regions, genes showing a normalised coverage value < 1E-8 in at least one line were
519 filtered out (12145 genes retained). As for RNA-seq, genes showing a CNV ≥ 1.5 fold (in either
520 direction) in the four pairwise 'resistant *vs* susceptible' comparisons were considered affected by
521 CNV in association with resistance.

522

523 *Long read sequencing and de novo assembly of the P450 duplication*

524 The genomic architecture of the duplicated locus was further examined in the duplicated IR0F line
525 versus the non-duplicated IR13 line. Both lines were submitted to long read sequencing using oxford
526 nanopore technology. Genomic DNA was extracted from pools of 75 adult females using the Gentra
527 Puregene Tissue kit (Qiagen) with 3 mL cell lysis buffer. Genomic DNA was quantified using Qubit
528 DNA Broad Range assay (Qiagen) and quality-checked by agarose gel electrophoresis before adjusting
529 concentration to 150 ng/µl. High genomic DNA fragments were selected using the Short Read
530 Eliminator kit (Circulomics). DNA libraries were prepared using 1 µg gDNA with the ligation
531 sequencing kit SQK-LSK109 kit (Oxford Nanopore) following manufacturer's instructions. Finally, 50
532 fmoles of the resulting DNA library were loaded on a R9.4.1 MinIon flow cell. Long read sequences
533 were collected from 2 independent runs of 48 h for each line. Sequencing generated a total of
534 515K/1017K reads with an average length of 13.5/9.8 Kb, representing 3.4/4.8-fold genome
535 coverage, for IR0F and IR13 lines respectively. Reads were mapped on the AaegL5 reference genome
536 using Winnowmap (Jain et al., 2022) and alignments were visualised using IGV (Robinson et al.,
537 2011). Finally, de novo genomes of the IR0F and IR13 lines were assembled using both Illumina short
538 reads and oxford nanopore long reads using MaSuRCA (Zimin et al., 2013). This de novo assembly
539 resulted into 17346/ 13160 contigs, with a median size of 40/55 kb for each line respectively.
540 Transposable elements were identified using BLAST against the RepBase library (10/12/2021
541 version).

542

543 *Quantification of the P450 duplication*

544 The detection of the P450 duplication was achieved through the quantification of *CYP6BB2* copy
545 number by digital droplet PCR (ddPCR). Genomic DNA was extracted from pools of mosquitoes using
546 the cetyltrimethylammonium bromide (CTAB) method (Collins et al 1987), resuspended in nuclease-
547 free water and quantified using Qubit DNA Broad Range assay (Qiagen). The duplex ddPCR
548 quantification assay was based on the co-amplification of two target genes each detected with
549 specific Taqman probes: the gene *CYP6BB2* (AAEL014893, Fam) was used to quantify the P450
550 duplication copy number while the gene *CYP4D39* (AAEL007808, Hex) always found as a single copy
551 in various *Ae. aegypti* lines was used as control for normalisation of gDNA quantities (Faucon et al.,
552 2015). Before amplification, gDNA samples were digested with XhoI for 15 min at 37°C directly within
553 the ddPCR reaction mixture. This reaction mixture was partitioned into up to 20,000 nanoliter-sized
554 droplets using the QX200 droplet generator (Bio-Rad) by mixing 70 µl of synthetic oil with 20 µl PCR

555 mix. Then, 40µL of the partitioned reaction was then amplified for 40 cycles with an annealing
556 temperature of 60°C (see **Supplementary file 8** for protocol details and primers/probes). After
557 amplification, the number of positive and negative droplets was quantified for both Fam and Hex
558 channels using the QX200 droplet reader (Bio-Rad) and the positive/negative ratio was used to
559 estimate the initial gDNA concentration of each gene assuming a Poisson distribution. After
560 normalisation for gDNA quantity, *CYP6BB2* copy number were expressed as mean copy number (±
561 95% CI).

562

563 *Quantification of the Ile1011Met kdr mutation frequency*

564 The frequency of the Ile1011Met kdr mutation was quantified on pools of mosquitoes using ddPCR.
565 Genomic DNA was extracted as described above and digested with XhoI for 15 min at 37°C before
566 partitioning. The duplex TaqMan reaction mixture contained two amplification primers together with
567 two Taqman probes labelled with Fam and Hex fluorophores corresponding to the Met and Iso alleles
568 respectively (see **Supplementary file 8** for protocol and primer/probes details). The duplex reaction
569 mixture was emulsioned as described above and amplified for 40 cycles with an annealing
570 temperature of 59°C. After droplet reading, the positive/negative ratio obtained for each channel
571 was visualised as a scatterplot and was used to estimate the frequency of each allele assuming a
572 Poisson distribution with 95% CI.

References

Achee, N. L., Grieco, J. P., Vatandoost, H., Seixas, G., Pinto, J., Ching-Ng, L., Martins, A. J., Juntarajumnong, W., Corbel, V., Gouagna, C., David, J.-P., Logan, J. G., Orsborne, J., Marois, E., Devine, G. J., & Vontas, J. (2019). Alternative strategies for mosquito-borne arbovirus control. *PLoS Negl Trop Dis*, *13*(1). https://doi.org/10.1371/journal.pntd.0006822

Anders, S., & Huber, W. (2010). Differential expression analysis for sequence count data. *Genome Biology*, *11*(10), R106. https://doi.org/10.1186/gb-2010-11-10-r106

Baker, M. D., Read, L. R., Beatty, B. G., & Ng, P. (1996). Requirements for Ectopic Homologous Recombination in Mammalian Somatic Cells. *Molecular and Cellular Biology*, *16*(12), 7122–7132. https://doi.org/10.1128/MCB.16.12.7122

Bariami, V., Jones, C. M., Poupardin, R., Vontas, J., & Ranson, H. (2012). Gene Amplification, ABC Transporters and Cytochrome P450s: Unraveling the Molecular Basis of Pyrethroid Resistance in the Dengue Vector, Aedes aegypti. *PLoS Negl Trop Dis*, *6*(6). https://doi.org/10.1371/journal.pntd.0001692

Bass, C., & Field, L. M. (2011). Gene amplification and insecticide resistance. *Pest Management Science*, *67*(8), 886–890. https://doi.org/10.1002/ps.2189

Benjamini, Y., & Hochberg, Y. (1995). Controlling the False Discovery Rate: A Practical and Powerful Approach to Multiple Testing. *J Royal Stat Soc B*, *57*, 289–300. https://doi.org/10.1111/j.2517-6161.1995.tb02031.x

Brengues, C., Hawkes, N. J., Chandre, F., McCarroll, L., Duchon, S., Guillet, P., Manguin, S., Morgan, J. C., & Hemingway, J. (2003). Pyrethroid and DDT cross-resistance in *Aedes aegypti* is correlated with novel mutations in the voltage-gated sodium channel gene. *Med Vet Entomol*, *17*(1), 87–94. https://doi.org/DOI: 10.1046/j.1365-2915.2003.00412.x

Brito, L. P., Carrara, L., Freitas, R. M. D., Lima, J. B. P., & Martins, A. J. (2018). Levels of Resistance to Pyrethroid among Distinct *kdr* Alleles in *Aedes aegypti* Laboratory Lines and Frequency of *kdr* Alleles in 27 Natural Populations from Rio de Janeiro, Brazil. *BioMed Research International*, *2018*, 1–10. https://doi.org/10.1155/2018/2410819

Brown, J. E., Evans, B. R., Zheng, W., Obas, V., Barrera-Martinez, L., Egizi, A., Zhao, H., Caccone, A., & Powell, J. R. (2014). Human impacts have shaped historical and recent evolution in *Aedes aegypti*, the dengue and yellow fever mosquito. *Evolution*, *68*(2), 514–525. https://doi.org/10.1111/evo.12281

Carvalho, V. L., & Long, M. T. (2021). Perspectives on New Vaccines against Arboviruses Using Insect-Specific Viruses as Platforms. *Vaccines*, *9*(3), 263. https://doi.org/10.3390/vaccines9030263

Cattel, J., Faucon, F., Le Peron, B., Sherpa, S., Monchal, M., Grillet, L., Gaude, T., Laporte, F., Dusfour, I., Reynaud, S., & David, J. P. (2020). Combining genetic crosses and pool targeted DNA-seq for untangling genomic variations associated with resistance to multiple insecticides in the mosquito Aedes aegypti. *Evolutionary Applications*, 303–317. https://doi.org/10.1111/eva.12867

Cattel, J., Haberkorn, C., Laporte, F., Gaude, T., Cumer, T., Renaud, J., Sutherland, I. W., Hertz, J. C., Bonneville, J., Arnaud, V., Fustec, B., Boyer, S., Marcombe, S., & David, J. (2021). A genomic amplification affecting a carboxylesterase gene cluster confers organophosphate resistance in the mosquito *Aedes aegypti*: From genomic characterization to high-throughput field detection. *Evolutionary Applications*, *14*(4), 1009–1022. https://doi.org/10.1111/eva.13177

Corbel, V., & N'Guessan, R. (2013). Distribution, Mechanisms, Impact and Management of Insecticide Resistance in Malaria Vectors: A Pragmatic Review, Anopheles mosquitoes -. *New insights into malaria vectors*. https://doi.org/10.5772/56117

David, J. P., Ismail, H. M., Chandor-Proust, A., & Paine, M. J. I. (2013). Role of cytochrome P450s in insecticide resistance: Impact on the control of mosquito-borne diseases and use of insecticides on Earth. *Philosophical Transactions of the Royal Society B-Biological Sciences*, *368*(1612). https://doi.org/10.1098/rstb.2012.0429

Djogbenou, L., Labbe, P., Chandre, F., Pasteur, N., & Weill, M. (2009). Ace-1 duplication in Anopheles gambiae: A challenge for malaria control. *Malar J*, *8*, 70. https://doi.org/10.1186/1475-2875-8-70

Dusfour, I., Thalmensy, V., Gaborit, P., Issaly, J., Carinci, R., & Girod, R. (2011). Multiple insecticide resistance in *Aedes aegypti* (Diptera: Culicidae) populations compromises the effectiveness of dengue vector control in French Guiana. *Mem Inst Oswaldo Cruz*, *106*(3), 346–352. https://doi.org/DOI: 10.1590/s0074-02762011000300015

Dusfour, I., Vontas, J., David, J. P., Weetman, D., Fonseca, D. M., Raghavendra, K., Corbel, V., Coulibaly, M., Martins, A. J., & Chandre, F. (2019). Management of insecticide resistance in the major Aedes vectors of arboviruses: Advances and challenges. *Plos Neg Trop Dis*, *13*(10), e0007615. https://doi.org/10.1371/journal.pntd.0007615

Dusfour, I., Zorrilla, P., Guidez, A., Issaly, J., Girod, R., Guillaumot, L., Robello, C., & Strode, C. (2015). Deltamethrin Resistance Mechanisms in Aedes aegypti Populations from Three French Overseas Territories Worldwide. *PLoS Negl Trop Dis*, *9*(11), e0004226. https://doi.org/10.1371/journal.pntd.0004226

Epelboin, Y., Wang, L., Giai Gianetto, Q., Choumet, V., Gaborit, P., Issaly, J., Guidez, A., Douché, T., Chaze, T., Matondo, M., & Dusfour, I. (2021). CYP450 core involvement in multiple resistance strains of Aedes aegypti from French Guiana highlighted by proteomics, molecular and biochemical studies. *PLOS ONE*, *16*(1), e0243992. https://doi.org/10.1371/journal.pone.0243992

Faucon, F., Dusfour, I., Gaude, T., Navratil, V., Boyer, F., Chandre, F., Sirisopa, P., Thanispong, K., Juntarajumnong, W., Poupardin, R., Chareonviriyaphap, T., Girod, R., Corbel, V., Reynaud, S., & David, J. P. (2015). Identifying genomic changes associated with insecticide resistance in the dengue mosquito Aedes aegypti by deep targeted sequencing. *Genome research*, *25*(9), 1347–1359. https://doi.org/10.1101/gr.189225.115

Faucon, F., Gaude, T., Dusfour, I., Navratil, V., Corbel, V., Juntarajumnong, W., Girod, R., Poupardin, R., Boyer, F., Reynaud, S., & David, J. P. (2017). In the hunt for genomic markers of metabolic resistance to pyrethroids in the mosquito *Aedes aegypti*: An integrated next-generation sequencing approach. *PLoS Negl Trop Dis*, *11*(4), e0005526. https://doi.org/10.1371/journal.pntd.0005526

Feyereisen, R., Dermauw, W., & Van Leeuwen, T. (2015). Genotype to phenotype, the molecular and physiological dimensions of resistance in arthropods. *Pesticide Biochemistry and Physiology*, *121*, 61–77. https://doi.org/10.1016/j.pestbp.2015.01.004

Ffrench-Constant, R. H., Daborn, P. J., & Le Goff, G. (2004). The genetics and genomics of insecticide resistance. *Trends Genet*, *20*(3), 163–170. https://doi.org/10.1016/j.tig.2004.01.003

Fontaine, A., Filipović, I., Fansiri, T., Hoffmann, A. A., Cheng, C., Kirkpatrick, M., Rašić, G., & Lambrechts, L. (2017). Extensive Genetic Differentiation between Homomorphic Sex Chromosomes in the Mosquito Vector, Aedes aegypti. *Genome Biology and Evolution*, *9*(9), 2322–2335. https://doi.org/10.1093/gbe/evx171

Garg, H., Mehmetoglu-Gurbuz, T., & Joshi, A. (2020). Virus Like Particles (VLP) as multivalent vaccine candidate against Chikungunya, Japanese Encephalitis, Yellow Fever and Zika Virus. *Scientific Reports*, *10*(1), 4017. https://doi.org/10.1038/s41598-020-61103-1

663 Goindin, D., Delannay, C., Gelasse, A., Ramdini, C., Gaude, T., Faucon, F., David, J. P., Gustave, J.,
664 Vega-Rua, A., & Fouque, F. (2017). Levels of insecticide resistance to deltamethrin, malathion, and
665 temephos, and associated mechanisms in Aedes aegypti mosquitoes from the Guadeloupe and
666 Saint Martin islands (French West Indies). *Infect Dis Poverty*, *6*(1), 38.
667 https://doi.org/10.1186/s40249-017-0254-x

668 Haddi, K., Tome, H. V. V., Du, Y., Valbon, W. R., Nomura, Y., Martins, G. F., Dong, K., & Oliveira, E. E.
669 (2017). Detection of a new pyrethroid resistance mutation (V410L) in the sodium channel of
670 *Aedes aegypti*: A potential challenge for mosquito control. *Scientific Reports*, *7*, 46549.
671 https://doi.org/10.1038/srep46549

672 Hawkins, N. J., Bass, C., Dixon, A., & Neve, P. (2018). The evolutionary origins of pesticide resistance.
673 *Biol Rev Camb Philos Soc*. https://doi.org/10.1111/brv.12440

674 Hemingway, J., Hawkes, N. J., McCarroll, L., & Ranson, H. (2004). The molecular basis of insecticide
675 resistance in mosquitoes. *Insect Biochemistry and Molecular Biology*, *34*(7), 653–665.
676 https://doi.org/10.1016/j.ibmb.2004.03.018

677 Hendry, A. P., Farrugia, T. J., & Kinnison, M. T. (2008). Human influences on rates of phenotypic
678 change in wild animal populations. *Molecular Ecology*, *17*(1), 20–29.
679 https://doi.org/10.1111/j.1365-294X.2007.03428.x

680 Hendry, A. P., Gotanda, K. M., & Svensson, E. I. (2017). Human influences on evolution, and the
681 ecological and societal consequences. *Philos Trans R Soc Lond B Biol Sci*, *372*(1712).
682 https://doi.org/10.1098/rstb.2016.0028

683 Hirata, K., Komagata, O., Itokawa, K., Yamamoto, A., Tomita, T., & Kasai, S. (2014). A single crossing-
684 over event in voltage-sensitive Na+ channel genes may cause critical failure of dengue mosquito
685 control by insecticides. *PLoS Negl Trop Dis*, *8*(8), e3085.
686 https://doi.org/10.1371/journal.pntd.0003085

687 Jain, C., Rhie, A., Hansen, N. F., Koren, S., & Phillippy, A. M. (2022). Long-read mapping to repetitive
688 reference sequences using Winnowmap2. *Nature Methods*, *19*(6), 705–710.
689 https://doi.org/10.1038/s41592-022-01457-8

690 Kasai, S., Itokawa, K., Uemura, N., Takaoka, A., Furutani, S., Maekawa, Y., Kobayashi, D., Imanishi-
691 Kobayashi, N., Amoa-Bosompem, M., Murota, K., Higa, Y., Kawada, H., Minakawa, N., Cuong, T. C.,
692 Yen, N. T., Phong, T. V., Keo, S., Kang, K., Miura, K., … Komagata, O. (2022). Discovery of super–
693 insecticide-resistant dengue mosquitoes in Asia: Threats of concomitant knockdown resistance
694 mutations. *Science Advances*, *8*(51), eabq7345. https://doi.org/10.1126/sciadv.abq7345

695 Kasai, S., Komagata, O., Itokawa, K., Shono, T., Ng, L. C., Kobayashi, M., & Tomita, T. (2014).
696 Mechanisms of pyrethroid resistance in the dengue mosquito vector, Aedes aegypti: Target site
697 insensitivity, penetration, and metabolism. *PLoS Negl Trop Dis*, *8*(6), e2948.
698 https://doi.org/10.1371/journal.pntd.0002948

699 Kondrashov, F. A. (2012). Gene duplication as a mechanism of genomic adaptation to a changing
700 environment. *Proceedings. Biological Sciences / The Royal Society*, *279*(1749), 5048–5057.
701 https://doi.org/10.1098/rspb.2012.1108

702 Kraemer, M. U., Sinka, M. E., Duda, K. A., Mylne, A. Q., Shearer, F. M., Barker, C. M., Moore, C. G.,
703 Carvalho, R. G., Coelho, G. E., Van Bortel, W., Hendrickx, G., Schaffner, F., Elyazar, I. R., Teng, H.-J.,
704 Brady, O. J., Messina, J. P., Pigott, D. M., Scott, T. W., Smith, D. L., … Hay, S. I. (2015). The global
705 distribution of the arbovirus vectors Aedes aegypti and Ae. Albopictus. *eLife*, *4*, e08347.
706 https://doi.org/10.7554/eLife.08347

707 Labbe, P., Berthomieu, A., Berticat, C., Alout, H., Raymond, M., Lenormand, T., & Weill, M. (2007).
708 Independent duplications of the acetylcholinesterase gene conferring insecticide resistance in the

mosquito Culex pipiens. *Mol Biol Evol*, *24*(4), 1056–1067. https://doi.org/10.1093/molbev/msm025

Li, X. C., Schuler, M. A., & Berenbaum, M. R. (2007). Molecular mechanisms of metabolic resistance to synthetic and natural xenobiotics. *Annual Review of Entomology*, *52*, 231–253. https://doi.org/10.1146/annurev.ento.51.110104.151104

Liu, N. (2015). Insecticide Resistance in Mosquitoes: Impact, Mechanisms, and Research Directions. *Annual Review of Entomology*, *60*(1), 537–559. https://doi.org/10.1146/annurev-ento-010814-020828

Lounibos, L. P. (2002). Invasions by insect vectors of human disease. *Annu Rev Entomol*, *47*, 233–266. https://doi.org/10.1146/annurev.ento.47.091201.145206

Marcombe, S., Carron, A., Darriet, F., Etienne, M., Agnew, P., Tolosa, M., Yp-Tcha, M. M., Lagneau, C., Yebakima, A., & Corbel, V. (2009). Reduced efficacy of pyrethroid space sprays for dengue control in an area of Martinique with pyrethroid resistance. *Am J Trop Med Hyg*, *80*(5), 745–751. https://doi.org/10.4269/ajtmh.2009.80.745

Marcombe, S., Darriet, F., Tolosa, M., Agnew, P., Duchon, S., Etienne, M., Yp Tcha, M. M., Chandre, F., Corbel, V., & Yebakima, A. (2011). Pyrethroid resistance reduces the efficacy of space sprays for dengue control on the island of Martinique (Caribbean). *PLoS Negl Trop Dis*, *5*(6), e1202. https://doi.org/10.1371/journal.pntd.0001202

Marcombe, S., Fustec, B., Cattel, J., Chonephetsarath, S., Thammavong, P., Phommavanh, N., David, J.-P., Corbel, V., Sutherland, I. W., Hertz, J. C., & Brey, P. T. (2019). Distribution of insecticide resistance and mechanisms involved in the arbovirus vector Aedes aegypti in Laos and implication for vector control. *PLOS Neglected Tropical Diseases*, *13*(12), e0007852. https://doi.org/10.1371/journal.pntd.0007852

Marcombe, S., Poupardin, R., Darriet, F., Reynaud, S., Bonnet, J., Strode, C., Brengues, C., Yebakima, A., Ranson, H., Corbel, V., & David, J.-P. (2009). Exploring the molecular basis of insecticide resistance in the dengue vector Aedes aegypti: A case study in Martinique Island (French West Indies). *BMC Genomics*, *10*. https://doi.org/494 10.1186/1471-2164-10-494

Martins, A. J., Brito, L. P., Linss, J. G., Rivas, G. B., Machado, R., Bruno, R. V., Lima, J. B., Valle, D., & Peixoto, A. A. (2013). Evidence for gene duplication in the voltage-gated sodium channel gene of Aedes aegypti. *Evolution, Medicine, and Public Health*, *2013*(1), 148–160. https://doi.org/10.1093/emph/eot012

Martins, A. J., Lins, R. M., Linss, J. G., Peixoto, A. A., & Valle, D. (2009). Voltage-gated sodium channel polymorphism and metabolic resistance in pyrethroid-resistant Aedes aegypti from Brazil. *Am J Trop Med Hyg*, *81*(1), 108–115. https://doi.org/10.4269/ajtmh.2009.81.108

Melo Costa, M., Campos, K. B., Brito, L. P., Roux, E., Melo Rodovalho, C., Bellinato, D. F., Lima, J. B. P., & Martins, A. J. (2020). Kdr genotyping in Aedes aegypti from Brazil on a nation-wide scale from 2017 to 2018. *Scientific Reports*, *10*(1), 13267. https://doi.org/10.1038/s41598-020-70029-7

Moyes, C. L., Vontas, J., Martins, A. J., Ng, L. C., Koou, S. Y., Dusfour, I., Raghavendra, K., Pinto, J., Corbel, V., David, J. P., & Weetman, D. (2017). Contemporary status of insecticide resistance in the major Aedes vectors of arboviruses infecting humans. *PLoS Negl Trop Dis*, *11*(7), e0005625. https://doi.org/10.1371/journal.pntd.0005625

Nene, V., Wortman, J. R., Lawson, D., Haas, B., Kodira, C., Tu, Z. J., Loftus, B., Xi, Z., Megy, K., Grabherr, M., Ren, Q., Zdobnov, E. M., Lobo, N. F., Campbell, K. S., Brown, S. E., Bonaldo, M. F., Zhu, J., Sinkins, S. P., Hogenkamp, D. G., … Severson, D. W. (2007). Genome sequence of *Aedes aegypti*, a major arbovirus vector. *Science*, *316*(5832), 1718–1723. https://doi.org/10.1126/science.1138878

Orr, H. A. (2005). The genetic theory of adaptation: A brief history. *Nat Rev Genet*, *6*(2), 119–127. https://doi.org/10.1038/nrg1523

Palumbi, S. R. (2001). Humans as the world's greatest evolutionary force. *Science*, *293*(5536), 1786–1790. https://doi.org/10.1126/science.293.5536.1786

Reid, W. R., Thornton, A., Pridgeon, J. W., Becnel, J. J., Tang, F., Estep, A., Clark, G. G., Allan, S., & Liu, N. (2014). Transcriptional Analysis of Four Family 4 P450s in a Puerto Rico Strain of *Aedes aegypti* (Diptera: Culicidae) Compared With an Orlando Strain and Their Possible Functional Roles in Permethrin Resistance. *Journal of Medical Entomology*, *51*(3), 605–615. https://doi.org/10.1603/ME13228

Remnant, E. J., Good, R. T., Schmidt, J. M., Lumb, C., Robin, C., Daborn, P. J., & Batterham, P. (2013). Gene duplication in the major insecticide target site, *Rdl* , in *Drosophila melanogaster*. *Proceedings of the National Academy of Sciences*, *110*(36), 14705–14710. https://doi.org/10.1073/pnas.1311341110

Riaz, M. A., Chandor-Proust, A., Dauphin-Villemant, C., Poupardin, R., Jones, C. M., Strode, C., Regent-Kloeckner, M., David, J.-P., & Reynaud, S. (2013). Molecular mechanisms associated with increased tolerance to the neonicotinoid insecticide imidacloprid in the dengue vector Aedes aegypti. *Aquatic Toxicology*, *126*, 326–337. https://doi.org/10.1016/j.aquatox.2012.09.010

Rigby, L. M., Rašić, G., Peatey, C. L., Hugo, L. E., Beebe, N. W., & Devine, G. J. (2020). Identifying the fitness costs of a pyrethroid-resistant genotype in the major arboviral vector Aedes aegypti. *Parasites & Vectors*, *13*(1), 358. https://doi.org/10.1186/s13071-020-04238-4

Robinson, J. T., Thorvaldsdóttir, H., Winckler, W., Guttman, M., Lander, E. S., Getz, G., & Mesirov, J. P. (2011). Integrative genomics viewer. *Nature Biotechnology*, *29*(1), 24–26. https://doi.org/10.1038/nbt.1754

Saavedra-Rodriguez, K., Campbell, C. L., Lozano, S., Penilla-Navarro, P., Lopez-Solis, A., Solis-Santoyo, F., Rodriguez, A. D., Perera, R., & Black Iv, W. C. (2021). Permethrin resistance in Aedes aegypti: Genomic variants that confer knockdown resistance, recovery, and death. *PLOS Genetics*, *17*(6), e1009606. https://doi.org/10.1371/journal.pgen.1009606

Saavedra-Rodriguez, K., Suarez, A. F., Salas, I. F., Strode, C., Ranson, H., Hemingway, J., & Black, W. C. th. (2012). Transcription of detoxification genes after permethrin selection in the mosquito Aedes aegypti. *Insect Mol Biol*, *21*(1), 61–77. https://doi.org/10.1111/j.1365-2583.2011.01113.x

Saavedra-Rodriguez, K., Urdaneta-Marquez, L., Rajatileka, S., Moulton, M., Flores, A. E., Fernandez-Salas, I., Bisset, J., Rodriguez, M., McCall, P. J., Donnelly, M. J., Ranson, H., Hemingway, J., & Black, W. C. (2007). A mutation in the voltage-gated sodium channel gene associated with pyrethroid resistance in Latin American *Aedes aegypti*. *Insect Molecular Biology*, *16*(6), 785–798. https://doi.org/doi: 10.1111/j.1365-2583.2007.00774.x.

Schrider, D. R., Houle, D., Lynch, M., & Hahn, M. W. (2013). Rates and Genomic Consequences of Spontaneous Mutational Events in *Drosophila melanogaster*. *Genetics*, *194*(4), 937–954. https://doi.org/10.1534/genetics.113.151670

Seixas, G., Grigoraki, L., Weetman, D., Vicente, J. L., Silva, A. C., Pinto, J., Vontas, J., & Sousa, C. A. (2017). Insecticide resistance is mediated by multiple mechanisms in recently introduced Aedes aegypti from Madeira Island (Portugal). *PLoS Negl Trop Dis*, *11*(7), e0005799. https://doi.org/10.1371/journal.pntd.0005799

Silva, J. V. J., Lopes, T. R. R., Oliveira-Filho, E. F. D., Oliveira, R. A. S., Durães-Carvalho, R., & Gil, L. H. V. G. (2018). Current status, challenges and perspectives in the development of vaccines against yellow fever, dengue, Zika and chikungunya viruses. *Acta Tropica*, *182*, 257–263. https://doi.org/10.1016/j.actatropica.2018.03.009

Smith, L. B., Kasai, S., & Scott, J. G. (2016). Pyrethroid resistance in *Aedes aegypti* and *Aedes albopictus*: Important mosquito vectors of human diseases. *Pesticide Biochemistry and Physiology*, *133*, 1–12. https://doi.org/10.1016/j.pestbp.2016.03.005

Uemura, N., Furutani, S., Tomita, T., Itokawa, K., Komagata, O., & Kasai, S. (2023). Concomitant knockdown resistance allele, L982W + F1534C, in Aedes aegypti has the potential to impose fitness costs without selection pressure. *Pesticide Biochemistry and Physiology*, *193*, 105422. https://doi.org/10.1016/j.pestbp.2023.105422

Valle, D., Bellinato, D. F., Viana-Medeiros, P. F., Lima, J. B. P., & Martins Junior, A. D. J. (2019). Resistance to temephos and deltamethrin in Aedes aegypti from Brazil between 1985 and 2017. *Memórias Do Instituto Oswaldo Cruz*, *114*, e180544. https://doi.org/10.1590/0074-02760180544

Weetman, D., Djogbenou, L. S., & Lucas, E. (2018). Copy number variation (CNV) and insecticide resistance in mosquitoes: Evolving knowledge or an evolving problem? *Curr Opin Insect Sci*, *27*, 82–88. https://doi.org/10.1016/j.cois.2018.04.005

WHO. (2022). *Standard operating procedure for testing insecticide susceptibility of adult mosquitoes in WHO tube tests. SOP version: WHO Tube test/01/14.* World Health Organization. https://iris.who.int/bitstream/handle/10665/352316/9789240043831-eng.pdf?sequence=1

Yanola, J., Somboon, P., Walton, C., Nachaiwieng, W., Somwang, P., & Prapanthadara, L. A. (2011). High-throughput assays for detection of the F1534C mutation in the voltage-gated sodium channel gene in permethrin-resistant *Aedes aegypti* and the distribution of this mutation throughout Thailand. *Trop Med Int Health*, *16*(4), 501–509. https://doi.org/10.1111/j.1365-3156.2011.02725.x

Zimin, A. V., Marçais, G., Puiu, D., Roberts, M., Salzberg, S. L., & Yorke, J. A. (2013). The MaSuRCA genome assembler. *Bioinformatics*, *29*(21), 2669–2677. https://doi.org/10.1093/bioinformatics/btt476

Zoh, M. G., Gaude, T., Prud'homme, S. M., Riaz, M. A., David, J.-P., & Reynaud, S. (2021). Molecular bases of P450-mediated resistance to the neonicotinoid insecticide imidacloprid in the mosquito Ae. Aegypti. *Aquatic Toxicology*, *236*, 105860. https://doi.org/10.1016/j.aquatox.2021.105860

Authors's contributions

JMB and JPD designed the study. TB, CH, JG, JC, MK, LN, TG, FL and JT performed experiments and analysed data. JF, FB, JV, JMB and JPD supervised data analysis. ID provided biological materials and data. JMB, JF and JPD acquired the funding. TB, JMB and JPD wrote and revised the paper.

Data availability

RNA-seq data have been deposited at EBI short read archive (SRA) under accession number E-MTAB-13325. DNA-seq short and long reads have been deposited at EBI short read archive (SRA) under accession number E-MTAB-13310.

Ethical aspects

Mice were kept in the animal facility of the Biology department of the University of Grenoble-Alpes, approved by the French Ministry of Animal Welfare (agreement no. B 38 421 10 001) and used in accordance with the laws of the European Union (directive 2010/63/EU). The use of animals for this study was approved by the ComEth Grenoble-C2EA-12 ethics committee mandated by the French Ministry of Higher Education and Research (MENESR). The study was conducted in accordance with the ARRIVE guidelines.

Aknowledgments

We thank the Institut Pasteur de La Guyane for providing the isofemale lines IR03 and IR13. We also thank Dr. Ademir Jesus Martins from the Fundación Oswaldo Cruz for a critical reading of the manuscript.

Funding

This study was partially supported by the European Union's Horizon 2020 research and innovation program under *ZIKAlliance* [grant agreement no. 734548]. This work was also supported by H2020 Research Infrastructures *Infravec2* [grant agreement no. 731060]. MK was supported a STMS fellowship funded by European Union's Horizon 2020 research and innovation under the *AIM COST action* [grant agreement no. CA17108]. The funders had no role in study design, data collection and interpretation, or decision to submit the work for publication.

856 # Figures

857 **Figure 1. Synergistic effect of PBO on deltamethrin resistance.** Adult females were exposed or not to
858 4% PBO for 1h followed by a 30-min exposure to 0.03% deltamethrin. Mortality was recorded 24h
859 after exposure. Mean mortality rates are indicated ± SD, and compared using a Wilcoxon test (N=5,
860 ns: not significant; **: p-value < 0.01).
861
862 **Figure 2. Genes over transcribed in resistant lines and their associated copy number variations.**
863 Only the 45 genes found significantly over transcribed from RNA-seq are shown (FC≥ 1.5 and
864 corrected P value ≤ 0.0005 in all resistant versus susceptible pairwise comparisons). Genes also
865 showing an elevated copy number from WG DNA-seq (FC ≥ 1.5) in all pairwise comparisons are
866 indicated with stars. Genomic coordinates (chromosome and start position), accession number and
867 description are indicated for all genes. Gene descriptions in grey were obtained from a BlastP against
868 NCBI Refseq. Genes in red belong to a single duplicated region on chromosome 1. Pool-seq read
869 coverage profiles of the susceptible IR13 and the resistant IR0F lines around the duplicated locus are
870 shown. Pie charts show the proportion of P450s in each dataset.
871
872 **Figure 3. Genomic architecture of the duplication.** The topology was deduced from both short and
873 long reads sequencing data. The six CYP6 genes carried by the duplication in the resistant lines are
874 represented by red arrows. Regions containing full or partial transposable elements are shown in
875 greater detail. Orange and yellow triangles denote the inverted terminal repeats from hAT (17 pb)
876 and PiggyBac-like (18 pb) elements respectively. Diagram is not to scale.
877
878 **Figure 4. Genotype-phenotype association study.** Genotype-phenotype association study. Left panel
879 shows mortality data obtained by exposing adult females from the IR0F and Bora-Bora lines and their
880 F1 and F2 progeny to 0.03% deltamethrin for 1 hour. Mean mortalities ± SD 24h after insecticide
881 exposure are shown and distinct letters indicate significant mortality differences (significant Kruskal-
882 Wallis test followed by post hoc Wilcoxon test with Bonferroni-Holm correction, N ≥ 5, p ≤ 0.05).
883 Middle and right panels show the copy number of *CYP6BB2* and the frequency of the *kdr* 1011Met
884 allele respectively as inferred by ddPCR on pools of individuals (mean ± 95% CI, Bora: N=19, IR0F:
885 N=23, F1: N=17, F2D: N=113, F2S: N=15). Dead and surviving F2 individuals 24h after insecticide
886 exposure are noted F2D and F2S respectively.
887
888 **Figure 5: Response of the P450 duplication and the *kdr* 1011Met allele to deltamethrin selection.**
889 Experimental evolution was performed from the F3 offspring of 'Bora-Bora x IR0F' reciprocal cross
890 using two replicate lines for each selection regime: deltamethrin-selection (SelA and SelB lines, black)
891 and no selection (NSA and NSB lines, grey). Circles and triangles distinguish replicates A and B. Grey
892 dashed lines indicate the generations for which Sel lines were selected with deltamethrin. Left panel
893 shows the resistance of each line as measured by bioassays with 0.03% deltamethrin (mean mortality
894 ± SD). Middle and right panels show the copy number of CYP6BB2 and the frequency of the kdr
895 1011Met allele respectively as inferred by ddPCR on pools of individuals (mean ± 95% CI, N ≥ 30). The
896 SelB *CYP6BB2* copy number data point marked with a '!' was caused by an unexpected sampling bias
897 and was therefore not included in the statistical analysis comparing *CYP6BB2* copy number between
898 Sel and NS lines across generation (Linear Mixed Effect Model, p=0.0088).

Supplementary materials

Supplementary file 1 (.tiff image). Bioassays data from F1 and F2 offspring used to investigate the mode of inheritance of the resistance phenotype. Top: Controlled crosses used to generate F1 and F2 individuals used for bioasays. Bottom: Comparative mortality data obtained from the Bora-Bora and IR0F lines together with the F1 and F2 progeny of each cross in males and females. Deltamethrin exposure conditions were 0.03% deltamethrin for 30 min for females and 0.015% deltamethrin for 25 min for males to account for their inherent lower insecticide tolerance. Mortality rates are indicated as mean ± SD. Distinct letters indicate significantly distinct means (Kruskal-Wallis test followed by post hoc pairwise Wilcoxon test with Bonferroni-Holm correction, N=5, $p \leq 0.05$).

Supplementary file 2 (.xlsx file). RNA-seq and CNV data sets. All protein coding genes showing a significant differential transcription (sheet 'RNA-seq') or a significant differential exonic coverage (sheet 'CNV') are shown. See methods for filtering conditions and thresholds. Gene descriptions beginning with a # were manually inferred from Blast X result.

Supplementary File 3 (.tiff image). Genomic architecture of the *kdr* locus in the IR0F resistant line. On chromosome 3, the 3' part of the VGSC gene, including the 21 last exons, is duplicated. Black bars indicate the position of the coding exons. The duplication is 125 Kb long, and is imperfect: the two copies, R and R' mostly differing in their intronic sequences. The duplication breakpoints, left (LB) and right (RB) are located at 315,905,811 bp and 316,030,250 bp on the reference genome AaegL5. The 1011Met codon is located on the upstream copy (R) and followed by a B type intron. The 1011Ile codon is on the downstream copy and followed by an A type intron (Martins et al, 2013). RNA-seq data supported the sole expression of the 1011Met allele.

Supplementary file 4 (.xlsx file). Long reads overlapping the P450 duplication breakpoints.

Supplementary file 5 (.docx file). Data supporting the identification of the transposable elements flanking the P450 duplication.

Supplementary file 6 (.docx file). RNA interference experiment. This document includes detailed results and methods.

Supplementary file 7 (.tiff image). Proposed evolutionary steps leading to the observed duplication architecture. Theoretical structures and those inferred from short and long reads data are indicated. The hAt-like and PiggyBac-like transposons are shown in purple and green respectively. Transposition events are shown as dashed lines. The second hAt-like transposition event would have created an incomplete copy of the hAT transposon, either directly or through a posterior deletion. Recombination events are shown as blue crossed lines. Stars indicates junctions that were confirmed by short reads data.

Supplementary File 8 (.docx file). Digital droplet PCR assays used to quantify the P450 duplication and the frequency of the Ile1011Met kdr mutation. This document provides all technical details related these ddPCR assays including amplification primers, TaqMan probes, PCR conditions and data interpretation.

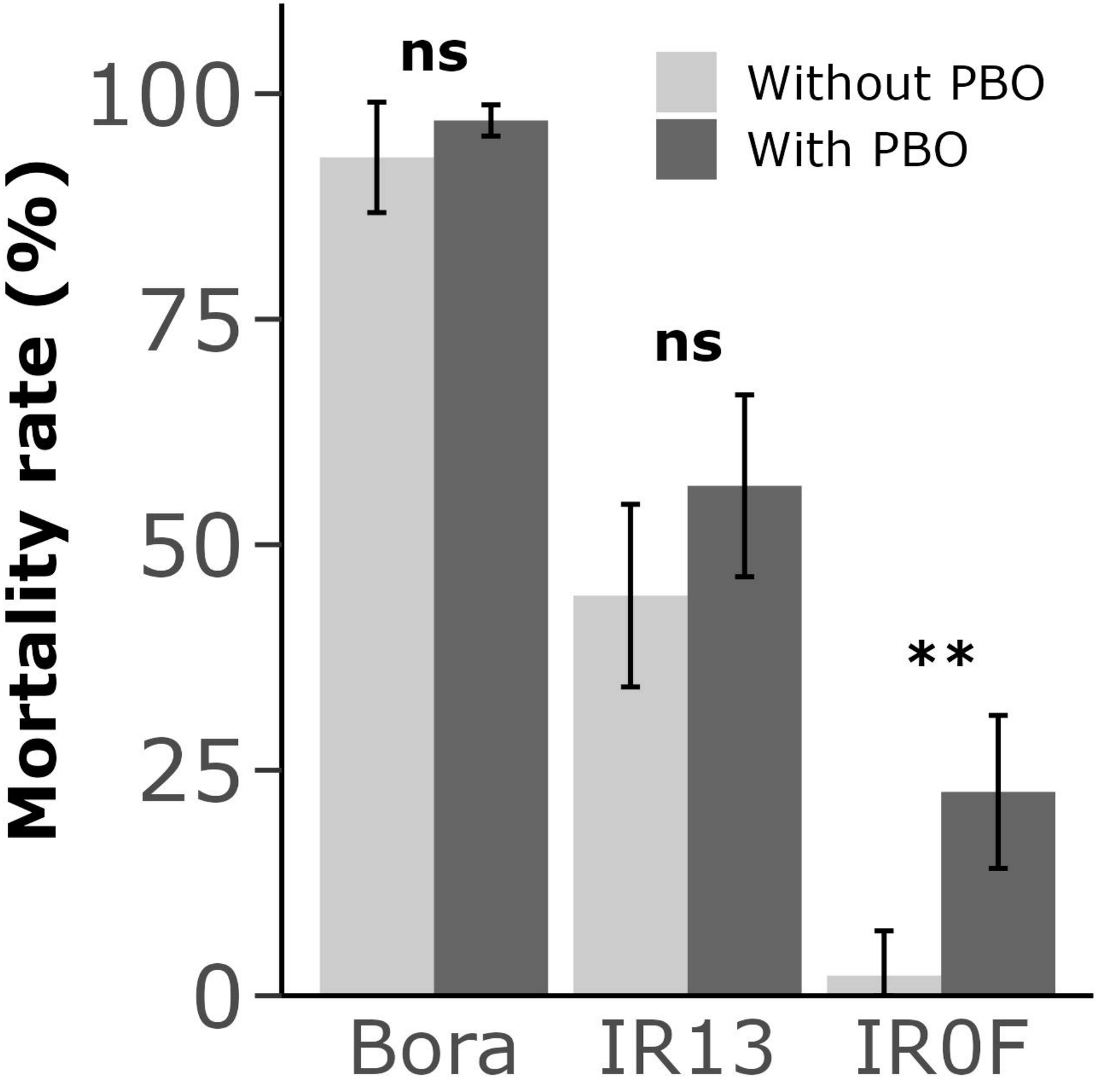
Mortality rate (%)
100
75
50
25
0
ns
ns
**
Without PBO
With PBO
Bora
IR13
IR0F

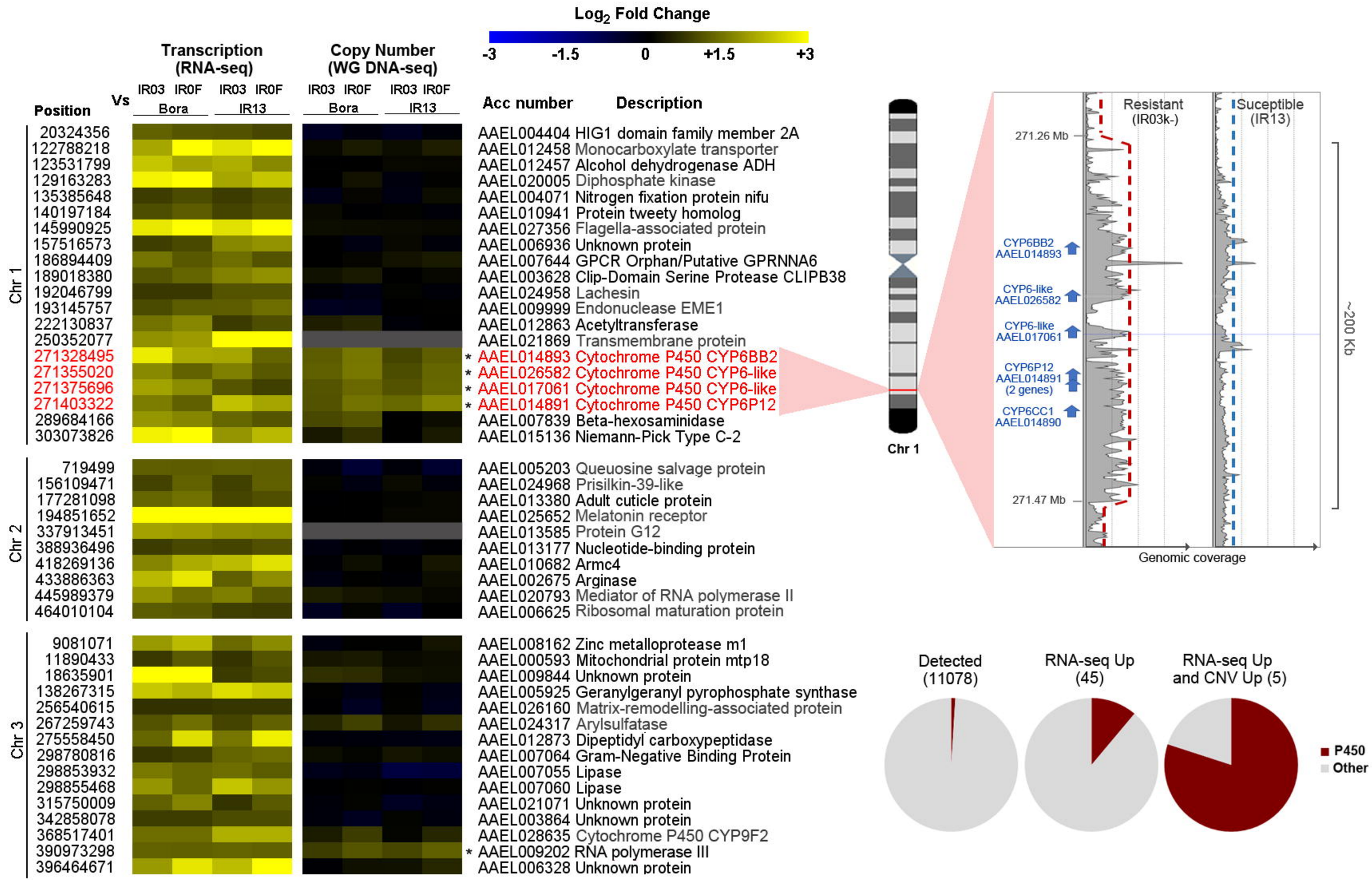
Log2 Fold Change
-3
-1.5
0
+1.5
+3
Transcription (RNA-seq)
Copy Number (WG DNA-seq)
Position
Vs
IR03 IR0F IR03 IR0F
Bora IR13
IR03 IR0F IR03 IR0F
Bora IR13
Acc number
Description
Chr 1
20324356 AAEL004404 HIG1 domain family member 2A
122788218 AAEL012458 Monocarboxylate transporter
123531799 AAEL012457 Alcohol dehydrogenase ADH
129163283 AAEL020005 Diphosphate kinase
135385648 AAEL004071 Nitrogen fixation protein nifu
140197184 AAEL010941 Protein tweety homolog
145990925 AAEL027356 Flagella-associated protein
157516573 AAEL006936 Unknown protein
186894409 AAEL007644 GPCR Orphan/Putative GPRNNA6
189018380 AAEL003628 Clip-Domain Serine Protease CLIPB38
192046799 AAEL024958 Lachesin
193145757 AAEL009999 Endonuclease EME1
222130837 AAEL012863 Acetyltransferase
250352077 AAEL021869 Transmembrane protein
271328495 * AAEL014893 Cytochrome P450 CYP6BB2
271355020 * AAEL026582 Cytochrome P450 CYP6-like
271375696 * AAEL017061 Cytochrome P450 CYP6-like
271403322 * AAEL014891 Cytochrome P450 CYP6P12
289684166 AAEL007839 Beta-hexosaminidase
303073826 AAEL015136 Niemann-Pick Type C-2
Chr 2
719499 AAEL005203 Queuosine salvage protein
156109471 AAEL024968 Prisilkin-39-like
177281098 AAEL013380 Adult cuticle protein
194851652 AAEL025652 Melatonin receptor
337913451 AAEL013585 Protein G12
388936496 AAEL013177 Nucleotide-binding protein
418269136 AAEL010682 Armc4
433886363 AAEL002675 Arginase
445989379 AAEL020793 Mediator of RNA polymerase II
464010104 AAEL006625 Ribosomal maturation protein
Chr 3
9081071 AAEL008162 Zinc metalloprotease m1
11890433 AAEL000593 Mitochondrial protein mtp18
18635901 AAEL009844 Unknown protein
138267315 AAEL005925 Geranylgeranyl pyrophosphate synthase
256540615 AAEL026160 Matrix-remodelling-associated protein
267259743 AAEL024317 Arylsulfatase
275558450 AAEL012873 Dipeptidyl carboxypeptidase
298780816 AAEL007064 Gram-Negative Binding Protein
298853932 AAEL007055 Lipase
298855468 AAEL007060 Lipase
315750009 AAEL021071 Unknown protein
342858078 AAEL003864 Unknown protein
368517401 AAEL028635 Cytochrome P450 CYP9F2
390973298 * AAEL009202 RNA polymerase III
396464671 AAEL006328 Unknown protein
Chr 1
Resistant (IR03k-)
Suceptible (IR13)
271.26 Mb
271.47 Mb
CYP6BB2 AAEL014893
CYP6-like AAEL026582
CYP6-like AAEL017061
CYP6P12 AAEL014891 (2 genes)
CYP6CC1 AAEL014890
~200 Kb
Genomic coverage
Detected (11078)
RNA-seq Up (45)
RNA-seq Up and CNV Up (5)
P450
Other

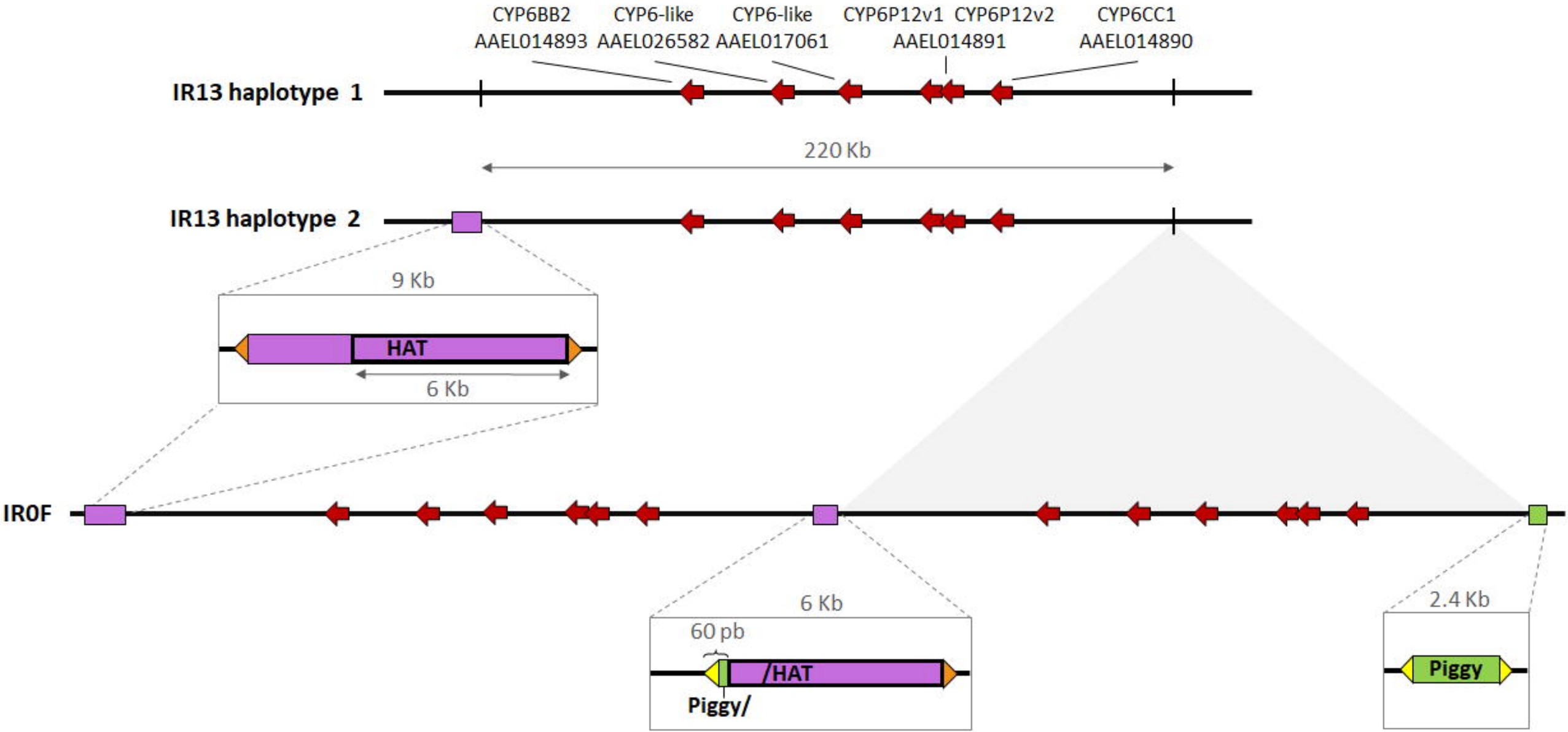
CYP6BB2
AAEL014893
CYP6-like
AAEL026582
CYP6-like
AAEL017061
CYP6P12v1
CYP6P12v2
AAEL014891
CYP6CC1
AAEL014890
IR13 haplotype 1
220 Kb
IR13 haplotype 2
9 Kb
HAT
6 Kb
IR0F
6 Kb
60 pb
/HAT
Piggy/
2.4 Kb
Piggy

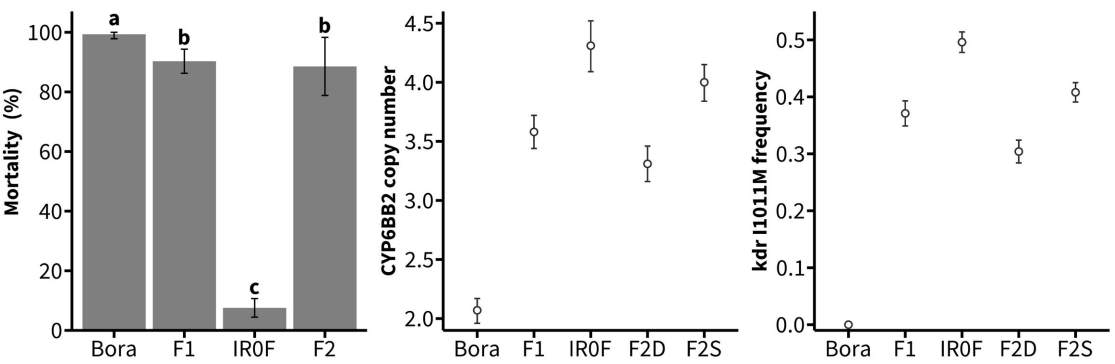
Mortality (%)
100
80
60
40
20
0
a
b
c
b
Bora
F1
IR0F
F2
CYP6BB2 copy number
4.5
4.0
3.5
3.0
2.5
2.0
Bora
F1
IR0F
F2D
F2S
kdr I1011M frequency
0.5
0.4
0.3
0.2
0.1
0.0
Bora
F1
IR0F
F2D
F2S

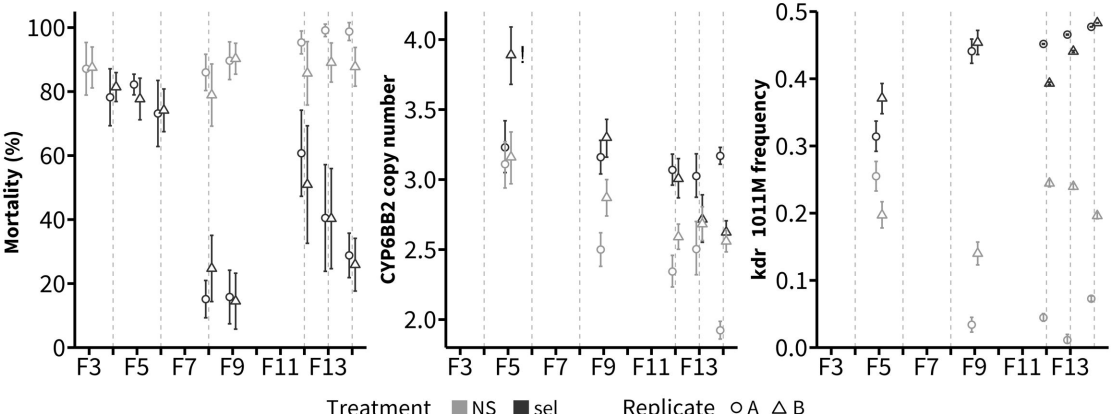
Mortality (%)
100
80
60
40
20
0
F3
F5
F7
F9
F11
F13
CYP6BB2 copy number
4.0
3.5
3.0
2.5
2.0
!
kdr 1011M frequency
0.5
0.4
0.3
0.2
0.1
0.0
Treatment
NS
sel
Replicate
A
B